Dual Fluorescence from Two Polar Excited States in One Molecule. Structurally Additive Photophysics of Crystal Violet Lactone

Jerzy Karpiuk*

Institute of Physical Chemistry, Polish Academy of Sciences, Kasprzaka 44/52, 01-224 Warsaw, Poland

Received: June 10, 2004; In Final Form: August 31, 2004

Crystal violet lactone (CVL) emits in aprotic solvents at room temperature single (A band, low polar solvents) or dual (A and B bands, medium and highly polar solvents) fluorescence. Strong solvatochromic shifts of both fluorescence bands prove significant charge redistribution in both emitting states (^1CT_A and ^1CT_B). Comparison with model compounds mimicking structural subunits of CVL, 6-dimethylaminophthalide (6-DMAPd), and malachite green lactone (MGL) shows that the A band is displayed from a polar excited state localized within the 6-DMAPd subunit (^1CT_A, $\mu_e \cong 10.7$ D), and the B band, from a highly polar excited state (^1CT_B, $\mu_e \cong 25.2$ D) formed after electron transfer from one of the dimethylaniline groups to 6-DMAPd moiety. The ^1CT_B state becomes accessible and is populated during solvation by a sufficiently polar environment. CVL phosphorescence strictly matches that of 6-DMAPd, indicating ISC to a triplet state localized on 6-DMAPd moiety in low polar solvents. In polar solvents, transient absorption measurements indicate spin flip and relaxation to a charge-transfer triplet state, as evidenced by identical $S_1 \rightarrow S_n$ and $T_1 \rightarrow T_n$ spectra in acetonitrile indicating presence of dimethylaniline cation radical. In protic media, CVL undergoes fast photodissociation of the C−O bond in lactone ring and diabatic formation of a zwitterion stabilized by hydrogen bonding with solvent molecule.

I. Introduction

The phenomenon of dual fluorescence emitted by organic molecules in solution is associated with a number of processes usually including photoinduced adiabatic reactions. Particular attention has been paid to dual fluorescence displayed in intramolecular electron transfer (ET) reactions accompanied by excited-state structural relaxation[1] where two fluorescence bands are emitted both from the substrate and the product of ET reaction (successor-precursor scheme). Eminent example is dual fluorescence of *N*,*N*′-dimethylaminobenzonitrile (DMABN) discovered by Lippert et al.[2] and interpreted within the framework of the TICT model proposed by Grabowski et al.[3] as coming from a locally excited (LE) state and from an intramolecular charge transfer (CT) state with electron-donating group twisted perpendicularly to the acceptor part. The TICT model has been successfully applied to describe photophysics of a large number of other flexible donor−acceptor (D−A) systems,[4,5] emphasizing the importance of mutually perpendicular D−A alignment for efficient charge separation (CS).

Another (much smaller) group of molecules includes those displaying dual fluorescence from two excited states, none of which can be identified with a vibrationally relaxed excited state of the primary excited molecule (i.e., the LE state). Such emitting states are products of a fast, multidimensional excited-state process and are populated on independent routes after branching into different adiabatic deactivation pathways.[6] The group includes i.a. systems built around spiro[7] carbon atom such as lactone forms of rhodamines (LRs).[4,8−10] LRs display dual fluorescence from (i) a highly polar ^1CT state, and (ii) from excited zwitterion (^1Z) formed in *adiabatic photodissociation* of the C−O bond in phthalide ring. Two relaxation channels leading to population of these states in LRs are triggered by ultrafast photoinduced intramolecular ET from bis(dimethyl)-xanthene to phthalide.

SCHEME 1

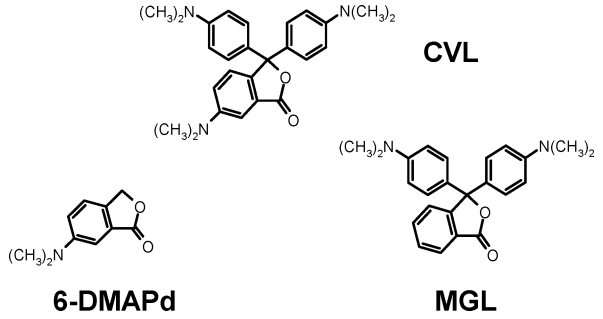

In contrast to LRs, where two dialkylaminophenyl groups are bridged into a rigid planar bis(dialkylamino)-xanthene forming a single π-electronic system, analogous lactone forms of triarylmethane dyes (LTAMs) have two individual electron-donating dialkylaniline groups forming a propeller-like structure with electron-accepting phthalide (Pd; Scheme 1). Despite structural difference when compared with analogous tetramethylrhodamine lactone (LRMET), malachite green lactone (MGL) displays single fluorescence from a CT state with electronic structure similar to that of the ^1CT state in LRs and the ^1CT state in MGL is populated in ET process faster than 130−150 fs.[11,12] Substitution of the phthalide moiety in MGL with the dimethylamino group gives another LTAM, crystal violet lactone (CVL, Scheme 1), and results in the complete change of photophysics and in dual fluorescence[13] in moderately and highly polar solvents. It seems that both the mechanism leading to the population of two emitting states in CVL and the nature of one of them are different from those in LRs, and

* To whom correspondence should be addressed. E-mail: karpiuk@ichf.edu.pl.

10.1021/jp0474935 CCC: $27.50
Published on Web 11/25/2004

the present paper attempts to resolve the intriguing puzzle of their origin. An important question is whether dual fluorescence of CVL is accompanied by structural relaxation involving, e.g., rotation of dialkylaniline groups. Though such structural change has been identified as the primary relaxation channel in excited triarylmethane cations[14] and was postulated in structurally related triphenylphosphine oxides,[15,16] it seems that structural changes play much less critical role in LTAMs photophysics.[11]

CVL is a colorless derivative of the well-known triarylmethane dye, crystal violet, and is important raw material for paper industry. CVL has been synthesized for the first time in an attempt to obtain a color former allowing a "carbonless" copy paper to be produced.[17] The process of color formation using CVL consists of a ground-state dissociation of the C−O bond in the lactone ring (in the presence of a proton donor) resulting in the formation of a crystal violet cation.[18,19] The lability of the C−O bond under various influences makes CVL very attractive for various applications, e.g., as photopolymerization initiator[20,21] and the active ingredient in thermochromic coatings.[22] In contrast to a vast number of studies on photophysics of TAM dyes,[23,24] and despite a widespread use of CVL, only a few studies have been carried out toward understanding the photophysics of CVL and other phthalide-based color formers.[25] The existing reports[20,26,27] give, however, incomplete or even misleading[20] insights into CVL spectroscopy. Moreover, intense work on the photodissociation of various leuco forms of triarylmethanes[28−35] and related 9-arylxanthenes[36,37] or fluorenols[38] surprisingly did not involve TAM lactones. It is more striking given the fact that adiabatic photodissociation in structurally related LR was reported by Grigoryeva et al.[9] as early as in 1977. Though Wan et al.[36] in their report on adiabatic photodehydroxylation in 9-phenylxanthen-9-ol critically assessed the possibility of adiabatic photoreactions in structurally similar amino-substituted triarylmethanols, Peters et al.[39] showed that photoinduced homolysis in diphenylmethylhalides results in the generation of radical pairs that are trapped in an electronic minimum on the excited state surface formed by avoided crossing of a covalent and an ionic surface. The formation of such radical pairs in LRs may be a key point in the population of the excited zwitterion state. For the above reasons, the study of LTAMs photophysics seemed both interesting and promising, especially with regard to insights it might provide into the complicated interactions of a nonrelaxed excited molecule with nonequilibrated solvent.

This paper presents the study of CVL photophysics and compares it with two compounds mimicking structural parts of CVL: 6-dimethylaminophthalide (6-DMAPd)[40] and malachite green lactone[11] (Scheme 1). Dual fluorescence displayed by CVL in more polar aprotic solvents comes from two polar excited states, one of which is localized within the 6-DMAPd part of the molecule, whereas the other is populated after ET from one of the dimethylaniline groups on the 6-DMAPd moiety. The medium surrounding the molecule plays a crucial role in CVL photophysics, with solvent polarity being the key factor affecting the energetics of both excited states and controlling availability of various deactivation pathways. The excited-state process in CVL in protic media involves formation of the cation following solvent assisted heterolytic cleavage of C−O bond in the lactone ring.

II. Experimental Section

CVL (Aldrich) was crystallized twice from acetone. MGL was synthesized as described by Fischer[41] and subsequently repeatedly recrystallized from *n*-propanol. 6-DMAPd was synthesized as described by Stanetty et al.[42] and purified by repeated crystallization from methanol. The solvents used were as follows: hexane (HEX), butyl ether (BE), ethyl ether (EE, inhibitor free), butyl acetate (BA), ethyl acetate (EA), tetrahydrofuran (THF), dichloromethane (DCM), 1,2-dichloroethane (DCE), pyridine (PY), acetone, benzonitrile (BZN), acetonitrile (ACN), dimethylformamide (DMF) and dimethyl sulfoxide (DMSO), methanol (MeOH), 1-propanol (PrOH), 1-butanol (BuOH), and 1-octanol (OcOH), and were all of spectroscopic grade. Butyronitrile (BTN, Merck) was triply distilled over $KMnO_4 + K_2CO_3$, P_2O_5, and CaH_2, respectively, and diisopropyl ether (IPE, p. a. Merck) was used as received. All luminescence measurements were carried out using solutions deoxygenated by saturation with purified and dried argon (30 min).

Absorption spectra were recorded with Shimadzu UV 3100 spectrophotometer, and emission measurements were carried out using an Edinburgh Analytical Instruments FS900 spectrofluorimeter. Luminescence spectra were subsequently corrected by subtraction of the background due to the solvent (e.g., Raman lines, excitation line passed as second order of monochromator grating). Fluorescence spectra were recorded as a function of wavelength and subsequently multiplied by a factor of λ^2 in order to convert counts per wavelength into counts per wavenumber. Luminescence quantum yields were determined using quinine sulfate in 0.1 N H_2SO_4 as a standard ($\Phi_f = 0.51$[43]) and corrected for the refractive index of a solvent.[44] For quantum yield determinations, optical densities of both the sample and the standard were identical at the wavelength of excitation and were of the order 0.1−0.15, which corresponded to CVL concentrations of about 4×10^{-5} to 6×10^{-5} M. Low-temperature luminescence measurements were carried out with a Jasny spectroflurimeter and phosphorimeter.[45] Phosphorescence was separated from total emission mechanically using a chopper system of the apparatus (modulation frequency of about 4 kHz). Luminescence lifetimes were obtained with an Edinburgh Analytical Instruments FL900 time-resolved fluorimeter. The χ^2 test and the distribution of residuals were the main criteria in evaluation of the quality of the fit.

Transient absorption measurements were carried out with a nanosecond transient absorption spectrophotometer constructed by Jasny[46] that allows for spectral measurements from 380 to 790 nm at delays ranging from −2 to 100 ns in relation to the excitation pulse (PTI PL 2300 nitrogen laser, fwhm = 0.6 ns, pulse energy 1 mJ), with a temporal resolution better than 1 ns.

Semiempirical quantum chemical AM1 calculations were performed with HYPERCHEM package (Hypercube Inc.).

III. Results and Their Interpretation

3.1. Absorption. The absorption spectra of CVL in three aprotic solvents and in methanol are shown in Figure 1. The spectra did not show any absorption in the 450−750 nm region, both before and after fluorescence measurements, indicating no presence of color ionic forms. Also a 2 h laser irradiation (337 nm, pulse energy 0.4 mJ, repetition rate 16 Hz) of a 5.9×10^{-4} M solution of CVL in ACN from freshly opened bottle (placed in a standard 1 cm × 1 cm fluorescence cell) did not result in any new absorption band.[47] The absorption spectra in alcohols did not indicate any specific ground-state interaction with the solvent.

The absorption spectrum of CVL in 200−450 nm region consists of four bands with the second band overlapped by a stronger third band. The lowest energy absorption band, ignored sometimes as a "tail",[27] shows large solvatochromic effect (1600 cm^{-1} red shift from hexane to DMSO). A comparison of CVL

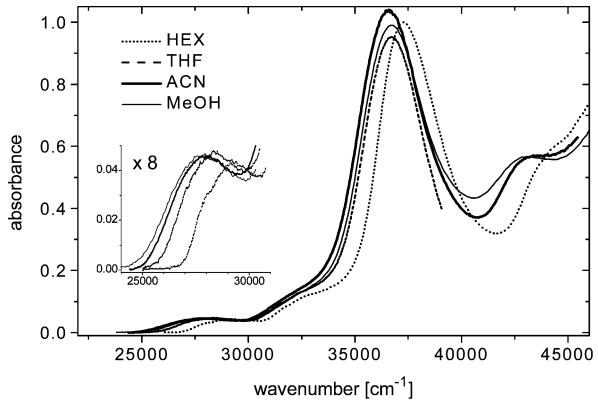

Figure 1. Absorption spectra of CVL in hexane (HEX, dotted line), tetrahydrofurane (THF, dashed line), acetonitrile (ACN, thick line), and methanol (MeOH, thin line). Insert shows solvatochromism of the first absorption band (note enlarged *Y* axis).

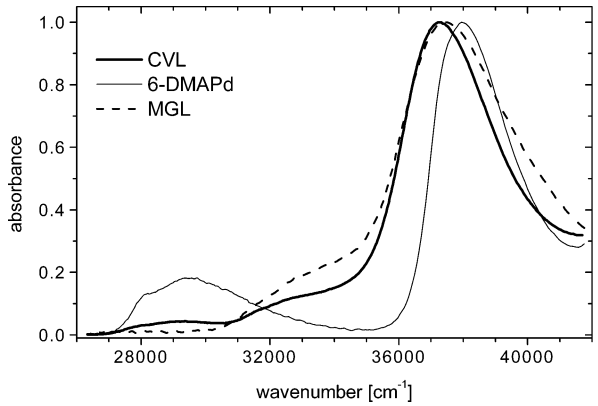

Figure 2. Comparison of the absorption spectrum of CVL with the spectra of compounds modeling its structural parts: 6-DMAPd and MGL. All of the spectra were recorded in hexane.

absorption spectrum in hexane with the spectra of compounds mimicking its structural parts, 6-DMAPd and MGL (Figure 2), shows that, whereas in MGL there is practically no absorption up to 30 000 cm^{-1}, the shapes of the lowest absorption bands and the spectral positions of their maxima in 6-DMAPd (29450 cm^{-1}) and in CVL (29300 cm^{-1}) are very similar, pointing to localization of the lowest absorbing state in CVL on the 6-DMAPd subunit. Moreover, virtually identical molar absorption coefficients at absorption maxima (e.g., 2550 and 2560 $M^{-1}cm^{-1}$, for 6-DMAPd and for CVL in ACN, respectively) suggest that the lowest absorption transition in CVL is very weakly perturbed by higher absorption transitions localized on DMA groups.

Such additivity of absorption transitions localized on structural subunits was reported for MGL[48] and for other leuco forms of triarylmethanes and was explained by weak conjugation of chromophores forming the molecule.[30] Though the solvatochromic red shift observed for the band in CVL (Table 1) is slightly larger than that for the corresponding band in 6-DMAPd, solvent effects in both CVL and 6-DMAPd clearly point to a charge-transfer nature of the lowest absorption transition in both molecules. AM1 semiempirical calculations for 6-DMAPd indicate that the $S_1 \leftarrow S_0$ transition involves significant displacement of charge density from the orbital localized on amino nitrogen to the orbital localized on the phenyl ring[40] and confirm earlier assignment in analogous 6-aminophthalide.[49] The low value of the absorption transition dipole moment in 6-DMAPd reflects a small overlap of molecular orbitals involved in the CT transition.

According to the theory of dielectric polarization,[50] a red shift of absorption band with increasing solvent polarity is expected for transitions from a state with a relatively small dipole moment to a state with a larger one. Localization of the lowest absorption transition in CVL on the 6-DMAPd moiety allows one to assume, to a rough approximation, a point dipole situated in the center of the spherical cavity created by the 6-DMAPd moiety.[51] Neglecting the mean solute polarizability in the states involved in the transition, the solvent effect on the spectral positions of the CT absorption spectra can be given by[52,53]

$$hc\tilde{\nu}_{abs} \cong hc\tilde{\nu}_{abs}^{vac} - \frac{2\vec{\mu}_g(\vec{\mu}_e - \vec{\mu}_g)}{a^3}\left[\frac{\epsilon - 1}{2\epsilon + 1} - \frac{1}{2}\frac{n^2 - 1}{2n^2 + 1}\right] \quad (1)$$

where $hc\tilde{\nu}_{abs}$ and $hc\tilde{\nu}_{abs}^{vac}$ are the energies related to the spectral positions of the CT absorption maxima in solutions and to the value extrapolated to the vacuum, respectively, $\vec{\mu}_g$ and $\vec{\mu}_e$ are the dipole moments of the solute in the ground and the excited states, respectively, a is the effective radius of the Onsager cavity,[54] ϵ is the static dielectric constant, and n is the refractive index of the solvent. For a well separated CT absorption band, eq 1 can be used to determine directly the values $\vec{\mu}_g(\vec{\mu}_e - \vec{\mu}_g)/a^3$ and $hc\tilde{\nu}_{abs}^{vac}$. Solvatochromic plots of absorption maxima for CVL and 6-DMAPd (see Supporting Information) yield practically equal $hc\tilde{\nu}_{abs}^{vac}$ energies in both molecules (3.70 eV), the slope, and consequently the $\vec{\mu}_g(\vec{\mu}_e - \vec{\mu}_g)/a^3$ value, are, however,

TABLE 1: Absorption and Fluorescence Data for CVL in Aprotic Solvents[a]

solvent	$\tilde{\nu}_{abs}^{CT}$ [cm^{-1}]	$\tilde{\nu}_{fl}^{CT}$(A) [cm^{-1}]	$\tilde{\nu}_{fl}^{CT}$(B) [cm^{-1}]	Φ_A	τ_A [ns]	k_r^A [$\times 10^{-7}$ s^{-1}]	k_{nr}^A [$\times 10^{-7}$ s^{-1}]	Φ_B	τ_B [ns]
HEX	29300	25850		.27	7.7	3.5	9.5		
BE	28850	25150		.39	12.3	3.2	5.0		
IPE	28870	25100		.41	13.7	3.0	4.5		
EE	28750	24450		.52	15.5	3.4	3.1		
BA	28600	24350		.51	21.9	2.3	2.2		
EA	28500	24100		.32	19.3	1.7	3.5		
THF	28350	24250		.44	22.4	2.0	2.5		
DCE	27950	23600	19600	.08	20.6			.12	20.7
PY	27800	23400	19000						
ACT		23400	18200		3.7				3.8
BZN	27850	23100	18600						
BTN	28050	23250	18100	.007	5.4			.025	5.7
DMF	27800	22100	17500	.0011	1.5			.0068	1.5
ACN	27950	22650	16950	.0006	1.5			.0039	1.4
DMSO	27700	21800	16500						

[a] $\tilde{\nu}_{abs}^{CT}$, absorption maximum; $\tilde{\nu}_{fl}^{CT}$(A) and $\tilde{\nu}_{fl}^{CT}$(B), maxima of fluorescence bands, A and B, respectively; Φ_A, Φ_B and τ_A, τ_B, fluorescence quantum yields and decay times of A and B bands, respectively; k_r^A and k_{nr}^A, radiative and nonradiative rate constants for the ^1CT_A state.

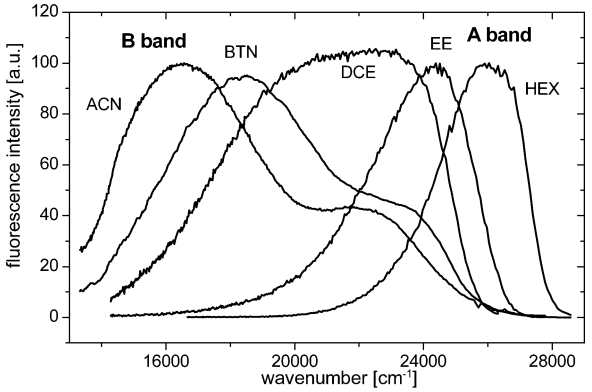

Figure 3. Fluorescence spectra of CVL in various aprotic solvents recorded at 295 K.

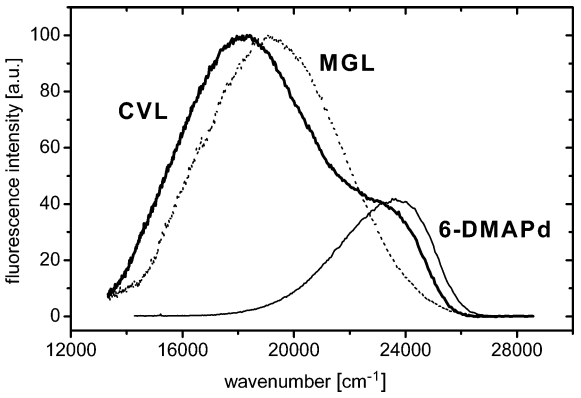

Figure 4. Fluorescence spectra of CVL, 6-DMAPd, and MGL in butyronitrile recorded at 295 K.

clearly larger for CVL (−0.32 eV) than for 6-DMAPd (−0.19 eV), indicating stronger solvent effect on absorption transition in CVL. $\vec{\mu}_e(\vec{\mu}_e - \vec{\mu}_g)/a^3$ values obtained from the plots of solvatochromic shifts of fluorescence maxima for both molecules are much closer to each other (−0.71 eV for 6-DMAPd and −0.66 eV for A band of CVL, see section 3.3), which suggests that the solvent effect on *emission* transitions in both molecules is about the same. Given that also emission in low polar solvents is displayed from excited state localized on 6-DMAPd part of CVL, the latter result suggests that Onsager cavity can be assumed nearly the same for 6-DMAPd standalone and 6-DMAPd as a component of CVL, and consequently, the above difference in $\vec{\mu}_g(\vec{\mu}_e - \vec{\mu}_g)/a^3$ values is not caused by different cavity radii, a, to be assumed for both situations but most probably is a consequence of a lower ground state dipole moment of 6-DMAPd as a component of CVL molecule due to (minor) inductive effects of dimethylaminophenyl groups. This is also reflected in ground state dipole moment AM1 calculations, yielding 5.9 D for 6-DMAPd and 5.5 D for CVL, with nearly the same dipole moment directions in both molecules.

The second (observed as a broad shoulder[55]) and the third absorption bands in CVL are similar to the first two bands in *N*,*N*′-dimethyl-*p*-toluidine[30] which models each of the two chromophores attached to 6-DMAPd and, contrary to rhodamine lactones,[56] are assigned to transitions localized within dimethylaniline units. Detailed description of higher absorption bands is given in the Supporting Information.

3.2. Fluorescence in Aprotic Solvents. Fluorescence spectra of CVL in aprotic solvents at room temperature show dramatic dependence on solvent polarity (Figure 3) and proticity (see section 3.5). In low polar aprotic solvents, CVL fluorescence spectra consist of one band shifting to the red on increasing solvent polarity. The shift is accompanied by increasing fluorescence quantum yield and longer fluorescence lifetime (Table 1). When the solvent polarity exceeds certain threshold value (at room-temperature somewhere above THF ($\epsilon = 7.6$) and below dichloromethane ($\epsilon = 8.9$)), a second fluorescence band appears and is emitted on further increase of solvent polarity. The appearance of the long-wave band is accompanied by significant decrease of both the short-wave band and the total fluorescence intensity. In the following, we will designate the short-wave band in CVL as the "A" band and the long-wave band as the "B" one, and we will denote the emitting states with respective letters.[57]

Fluorescence excitation spectra recorded in various solvents with fluorescence monitored in each of two fluorescence bands overlap with each other and reproduce well the CVL absorption spectrum, so that both bands are to be ascribed to emissions from CVL molecule. The long-wave band is emitted definitely from a different electronic state than the short-wave one. Considerable red shifts in spectral positions of both CVL luminescence bands, increasing Stokes shifts and bandwidths (fwhm) on increasing solvent polarity strongly suggest polar, charge-transfer nature of both emitting states. For that reason, the two emitting states will be referred to in the following as ^1CT_A and ^1CT_B excited states, respectively. The decay times measured in both emission bands (excitation at 337 nm) in a given solvent were found to be approximately equal on the ns time scale used in measurements (Table 1). No rising components have been detected for either A or B band on the sub-ns time scale. In solvents where CVL displays dual fluorescence, the decay times were measured at the blue and the red slopes of A and B bands, respectively, to avoid any spectral overlap of A and B bands (see Figure 4). Radiative and nonradiative rate constants for CVL in low polar solvents (k_r and k_{nr}, Table 1) have been determined assuming that 100% of primarily excited CVL molecules relax to solvent-equilibrated ^1CT_A state and the ^1CT_B state is not populated.

The fluorescence spectrum of CVL in ACN consisting apparently of two bands has been reported by Kaneko and Neckers,[20] without, however, any indication of its dual nature. The short-wave band in their spectrum has a maximum coinciding approximately with that reported here (about 430 nm as read out form Figure 3 in ref 20), but the long-wave band has a maximum at 541 nm (compared with 574 nm in our case) and apparently smaller spectral half-width than that found here. Using a 8.3×10^{-4} M solution of CVL in ACN (the concentration used in ref 20), it has been verified in this work that the discrepancy cannot result from relatively high CVL concentration used in ref 20, which would imply that the spectrum published by Kaneko and Neckers might, e.g., have not been appropriately corrected for the spectral response of their detection system. Also the fluorescence quantum yields given by these authors should be taken with care, as they give no details concerning the use of rhodamine B as an actinometer, and rhodamine B is well-known for variations of reported quantum yield and its dependence on various factors.[58]

The localization of the lowest excited state of CVL (in absorption) on the 6-DMAPd moiety strongly suggested that one of the fluorescence bands may correspond to a transition localized on that CVL subunit.[40] A comparison of spectral position and width of fluorescence band of 6-DMAPd with the short-wave fluorescence band recorded for CVL in the same solvent (Figure 4) strongly indicates that both emissions come essentially from the same chromophore. Near-mirror symmetry

of reduced absorption ($\epsilon(\nu)/\nu$ plotted versus ν) and reduced emission ($I(\nu)/\nu^3$ plotted versus ν) spectra[59] of CVL in low polar solvents proves that both the first absorption band and the fluorescence band represent transition to (absorption) or from (emission) a single and the same electronic state (see the Supporting Information for details). Almost equal absorption and emission transition dipole moments for 6-DMAPd in low polar solvents (e.g., in butyl ether $M_{abs} = 1.5$ D and $M_{flu} = 1.6$ D) indicate that vibrational relaxation is not accompanied by significant conformational changes in the 6-DAMPd moiety and that the Stokes shifts reflect mainly energetics of solvation of that part of the molecule, resembling the photophysics of coumarin 153.[60]

Stokes shifts, solvatochromic shifts, and half-widths of the long-wave B band of CVL are significantly larger than those of the A band, indicating that the band is displayed from a state much more polar than ^1CT_A. Unlike rhodamine lactones,[9] the shape and spectral position of the B band in CVL excludes its origin from a possible zwitterionic structure (**Z**), which would be formed after an adiabatic photodissociation of the C−O bond in the phthalide ring, as the long-wave CVL emission occurs at higher energies than the absorption band of the **Z** form.[61] Instead, the B band in CVL resembles the broad CT band observed in lactonic forms of rhodamines as their short-wave fluorescence[8] and interpreted as coming from the highly polar CT state with electron transferred from the bis(dimethylamino)-xanthene to the phthalide unit.[8,10,56] On the other hand, the B band in CVL is very similar to the fluorescence band observed in MGL in the same solvent in terms of half-width, spectral position, and solvatochromic shift of fluorescence maximum (cf. Figure 4 and the Supporting Information). This spectral similarity implies that the two bands come from excited states with very similar electronic structures. The fluorescence of MGL shows a very large Stokes shift (exceeding 16 000 cm^{-1} in DMSO) and a strong solvatochromic effect and has been assigned to a highly polar CT state with an electron transferred from the dimethylaminophenyl ring of the molecule to the phthalide moiety.[11] In light of these analogies between CVL and MGL the same conclusion holds for CVL.

For 6-DMAPd, the fluorescence quantum yield and lifetime increase gradually with solvent polarity from 0.38 and 7.9 ns, respectively, in HEX, through 0.69 and 25.1 ns, respectively, in THF, to 0.73 and 39.2 ns, respectively, in ACN (k_r changes correspondingly from 4.8×10^7 s^{-1} in HEX through 2.7×10^7 s^{-1} in THF to 1.9×10^7 s^{-1} in ACN). Nearly constant in absorption ($M_{abs} = 1.5-1.6$ D), the transition dipole moments in emission (M_{fl}) decrease from 1.8 D in HEX to 1.0 D in ACN. Lower emission probability and slowing down of the nonradiative decay (k_{nr} decreases by an order of magnitude from HEX to ACN) point out to a durable charge displacement in the excited state in 6-DMAPd with increasing solvent polarity.[40]

In low and medium polarity solvents, the quantum yield and the lifetime of A luminescence in CVL increase gradually from 0.27 and 7.7 ns, respectively, in hexane to 0.44 and 22.4 ns, respectively, in THF. This would correspond to a similar decrease in k_r and M_{fl} on increasing solvent polarity (Table 1) as in 6-DMAPd, assuming that only the ^1CT_A state is populated in solvents with a dielectric constant between HEX and THF (the ^1CT_B state being energetically not accessible). Showing the same growing trend, the fluorescence quantum yield of CVL is, however, distinctly lower than that of 6-DMAPd, indicating higher efficiency of nonradiative deactivation of the ^1CT_A state in 6-DMAPd as a CVL component than in the 6-DMAPd molecule due to enhanced ISC in CVL in low and medium polar solvents (see section 3.6).

Energetic stabilization and availability of the highly polar ^1CT_B state in more polar solvents is accompanied by dramatic decrease in total CVL fluorescence quantum yield by several orders of magnitude (e.g., down to 0.0045 in ACN). To separate both fluorescence bands and to determine the quantum yields of A and B fluorescences of CVL as well as the spectral positions of their maxima, a procedure for decomposing the luminescence spectrum into two bands has been applied assuming that the shapes of A and B bands are the same as those for 6-DMAPd and MGL in given solvent, respectively (see Supporting Information). The quantum yields of A and B luminescences and the positions of their maxima obtained using the above decomposition procedure are given in Table 1.

3.3. Excited-State Dipole Moments (Aprotic Solvents). Polar nature of the emitting excited states has been verified by estimating their dipole moments with solvatochromic shift method. Numerous variations of the method that exist in the literature are based on the reaction field model developed by Onsager,[54] which considers a solute molecule as a point dipole situated in a center of a spherical cavity formed by solvent molecules surrounding the solute molecule and interacting with its dipole via the reaction field. Applying Onsager model to a molecule composed of (nearly) noninteracting chromophores with a dipole moment localized mainly on one of them one may confine the Onsager cavity to a direct surrounding of that specific part of the molecule.[62,63] This seems to be justified as mainly the solvent molecules forming the cavity around the part of the solute where the dipole moment is changed upon electronic transition are displaced to create a new reaction field in the cavity. Thus, before attempting to estimate the dipole moments of the two excited states in CVL from solvatochromic plots of fluorescence maxima, additional assumptions concerning the cavity radii for both emitting states are to be made to account for the fact that the excited state displaying A luminescence is localized on the 6-DMAPd moiety, and the excited state displaying B band is distributed over the bis(dimethylanilino) and the 6-DMAPd parts of the molecule. These spatial arrangements of the two excited states have to be reflected in effective radii of the spherical Onsager cavities to be assumed for both emitting states in the analysis of solvatochromic plots, as both excited states have different distributions of charge density and subsequently differently polarize surrounding solvent molecules. Therefore, it seemed reasonably to assume that spherical Onsager cavities for both emitting states (and their radii, a_A and a_B, respectively) are different and are formed by solvent molecules surrounding only that part of the molecule which is directly involved in the radiative CT process in emission: 6-DMAPd moiety for the A state and the entire CVL molecule for the B state. The above had also to be appropriately taken into account in ground-state dipole moments assumed in the analysis of solvatochromic plots (see below).

As the measured lifetimes of fluorescent states are much longer than the solvent orientational relaxation times, the excited-state dipole moments can be estimated from the solvent effect on spectral position of fluorescence maxima using Lippert−Mataga[64] approach modified for fluorescence maxima.[65] The shifts of fluorescence maxima were chosen in view of the comparison with MGL, where estimation of the excited-state dipole moment from the solvent effect on the Stokes shift was not possible, as the emitting CT state was not that reached in absorption and the same holds for the CT_B state in CVL. Assuming a point dipole moment situated in a center of a

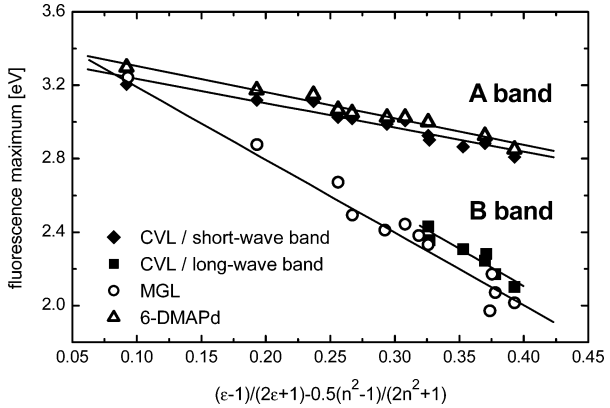

Figure 5. Solvatochromic shifts of fluorescence maxima for both (A and B) CVL bands as a function of solvent polarity corresponding to modified Lippert−Mataga model (eq 2), compared with those for 6-DMAPd and MGL.

TABLE 2: Slopes of the Fluorescence Solvatochromic Plots for CVL A and B Bands, 6-DMAPd, MGL (acc. to Eq 2), and the Dipole Moments Calculated for the Respective Excited States

	CVL/A	6-DMAPd	CVL/B	MGL[a]
$\vec{\mu}_e(\vec{\mu}_e - \vec{\mu}_g)/a^3$ [eV]	−0.66	−0.71	−2.04	−2.0
$hc\nu_{flu}^{vac}$ [eV]	3.37	3.45	3.74	3.61
μ_e [D]	10.7[b]	9.7[b]	25.2[c]	25.0[c]

[a] data for MGL taken from ref 11. [b] $a = 3.6$ Å. [c] $a = 5.8$ Å.

spherical cavity and neglecting the mean solute polarizability in the states involved in the transition, the following expression for solvent-equilibrated fluorescence maximum, $\tilde{\nu}_{fl}$, can be used:

$$hc\tilde{\nu}_{fl} \cong hc\tilde{\nu}_{fl}^{vac} - \frac{2\vec{\mu}_e(\vec{\mu}_e - \vec{\mu}_g)}{a^3}\left[\frac{\epsilon - 1}{2\epsilon + 1} - \frac{1}{2}\frac{n^2 - 1}{2n^2 + 1}\right] \quad (2)$$

where $\vec{\mu}_g$ and $\vec{\mu}_e$ are the dipole moments of the solute in the ground and the excited states, respectively, $\tilde{\nu}_{fl}^{vac}$ is the spectral position of fluorescence maximum in the gas phase and a is the effective radius of the Onsager cavity. ϵ is the static dielectric constant, and n is the refractive index of the solvent. Figure 5 shows fluorescence maxima plotted as a function of solvent polarity $f(\epsilon, n) = (\epsilon - 1)/(2\epsilon + 1) - 0.5(n^2 - 1)/(2n^2 + 1)$ for both CVL bands compared with those for 6-DMAPd and MGL. Good linear correlations between $hc\tilde{\nu}_{fl}$ and the solvent polarity function allow one to determine directly the values $\vec{\mu}_e(\vec{\mu}_e - \vec{\mu}_g)/a^3$ (Table 2), from which μ_e values can be estimated.

Excited-State Emitting A Band. Very close parameters of solvatochromic plots for A band of CVL and for 6-DMAPd (Table 2, Figure 5) indicate similar dipole moments of corresponding emitting states in both molecules. Exact determination of the excited-state dipole moment value, μ_e, from eq 2 would require the Onsager cavity radius a, the ground-state dipole moment, $\vec{\mu}_g$, and the angle between $\vec{\mu}_e$ and $\vec{\mu}_g$, α. Appropriate estimation of a value has critical impact on final uncertainty of μ_e as a enters the equations to the third power. Due to lack of crystal structure data on dimethylaminophthalides, a value for 6-DMAPd was estimated from geometrical parameters calculated with AM1 method. It is to be noted that significantly different approaches to estimate a from molecular dimensions in structurally related molecules have been proposed, ranging from a half of the maximum distance across which charge separation occurs in aminophthalimides[66] to using 40% of the long molecular axis obtained from ground-state molecular geometry and adding of van der Waals radii in 7-aminocoumarines.[67] a values estimated with these two approaches for 6-DMAPd were as different as 3.0 and 4.1 Å.[68] In our estimation, Onsager cavity radius a_A (for the ^1CT_A state) is assumed to be a half of the distance between the carbon atom from methyl group attached to amino nitrogen and the oxygen in the lactone ring in 6-DMAPd (3.6 Å), which is a compromise between two extreme values given above. AM1 calculations of μ_g for 6-DMAPd yielded $\mu_g = 5.9$ D and for CVL $\mu_g = 5.5$ D. The difference $\Delta\mu_{eg} = |\vec{\mu}_e - \vec{\mu}_g|$ could be calculated from the plot of Stokes shifts vs solvent polarity function[52] ($\Delta\mu_{eg} = 6.1$ D for $a = 3.6$ Å). The estimation based on the Stokes shift dependence on solvent polarity can be used for A band, as ^1CT_A state is directly populated in absorption. Calculating the angle between $\vec{\mu}_g$ and $\Delta\vec{\mu}_{eg}$ vectors, β, from the product $\vec{\mu}_g(\vec{\mu}_g - \vec{\mu}_e)$ determined from the slope of the plot of absorption maxima vs solvent polarity function (−0.2 eV) one can easily obtain the μ_e value and the angle α between $\vec{\mu}_g$ and $\vec{\mu}_e$.[69] With that calculation, it has been found for 6-DMAPd that $\mu_e = 9.7$ D and $\alpha \approx 32°$.[70] Though the absolute μ_e value is not as high as for, e.g., TICT states with full charge separation in molecules of comparable size,[71] it is significantly larger and angularly displaced as compared with $\vec{\mu}_g$. Furthermore, $\Delta\mu_{eg}$ reaches similar value as that reported recently for coumarine 153 (7.1 D)[72] where significant charge displacement has been claimed.

Ground-state dipole moment for CVL obtained from AM1 calculation is equal to 5.5 D and directed similarly as in 6-DMAPd. Using the same assumptions and procedure for A band of CVL as applied for 6-DMAPd above, and assuming for ^1CT_A state a spherical Onsager cavity confined to 6-DMAPd moiety with the same radius as for 6-DMAPd, one obtains for ^1CT_A in CVL μ_e^A equal to 10.7 D and $\alpha \approx 14°$. In view of an excellent agreement of the solvatochromic plots for 6-DMAPd and for CVL short-wave band, this somewhat larger value and smaller angle than those found for 6-DMAPd indicate some inductive effect of DMA groups in less polar solvents. Nevertheless, both μ_e values strongly support the conclusion on similar electronic configuration in the excited state of 6-DMAPd and in ^1CT_A state in CVL.

Excited-State Emitting B Band. In view of much stronger solvent effect on the B band and, consequently, much more polar nature of CT_B state, in calculation of μ_e^B, μ_g was assumed to be much less than μ_e^B and neglected,[73] as for MGL.[11] As the CT_B state extends over the entire molecule, Onsager cavity was assumed to comprise the entire CVL molecule. The Onsager cavity radius, a_B, was estimated to be an average distance from the central carbon atom to amino nitrogens and equal to 5.8 Å. The same value was also used previously for MGL molecule. With these assumptions, excited-state dipole moments for CVL (CT_B state) and for MGL, calculated from solvatochromic shifts of fluorescence maxima, are equal to 25.2 and 25.0 D, respectively. Also in this case, excellent agreement of the slopes of solvatochromic plots for CVL and MGL (Figure 5) proves similar electronic structures of both excited states.

3.4. Temperature Measurements and Phosphorescence. Fluorescence spectra of CVL in liquid BTN as a function of temperature are shown in Figure 6. It has been verified in temperature-dependent absorption measurements that the change in absorbance of CVL solution with decreasing temperature is to be ascribed to the solvent contraction only, so that the changes in fluorescence intensities directly reflect those of fluorescence quantum yields.[74] Gradual decrease in total intensity is accompanied by significant red shift of the long-wave band from 18 100 cm^{-1} at 295 K to 16 900 cm^{-1} at 173 K. The shift results from an increase of BTN polarity on decreasing temperature

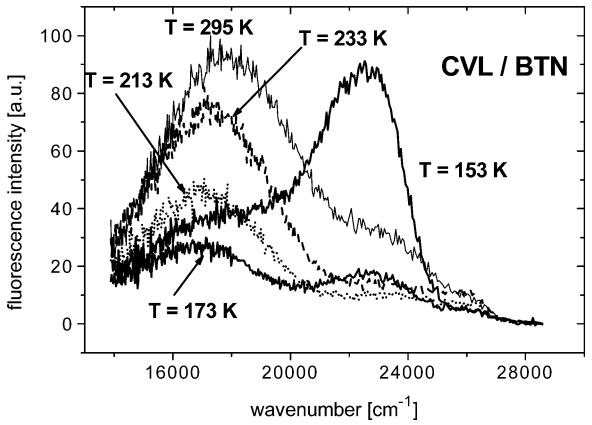

Figure 6. CVL luminescence spectra as a function of temperature in BTN.

and is comparable to that observed for MGL under similar conditions.[11] The change of BTN dielectric constant with temperature can be estimated using the formula $\epsilon(T) = -8.34 + 9724(1/T)$.[75] At 213 K, $\epsilon_{BTN} = 37.3$ and practically equals to that of acetonitrile at 293 K (37.5).[76] The positions of fluorescence maxima and the shape of CVL spectrum in BTN at 213 K match very well those observed for CVL in ACN at room temperature, proving that the energies of the ^1CT_B state in different media are essentially equal under *isopolar* conditions, and the same holds for ^1CT_A. Differences in fluorescence quantum yields determined for these two situations (total $\Phi_{fl} = 0.0045$ for ACN at 295 K and total $\Phi_{fl} = 0.013$ for BTN at 213 K) indicate that another solvent parameter (property) must control either (i) the initial transition from ^1CT_A to ^1CT_B state, thus affecting the yield of ^1CT_B state formation, or (ii) the kinetics of the deactivation process from ^1CT_B state under these isopolar conditions. The present paper does not provide, however, sufficient data to discuss (i) question and a more refined time-resolved study must address the issue. Possible mechanisms of nonradiative process are discussed below.

Decreasing temperature of CVL solution in BTN (up to 193 K) resulted in lowering of the total fluorescence quantum yield and in decreasing of Φ_A in relation to Φ_B, accompanied by red shifts of both bands. Below 193 K,[77] Φ_A begins to increase, and its growth, down to 153 K, is accompanied by decreasing of the B band and by further red shifts of both bands. The red shifts reflect the increase in BTN polarity in that temperature range, and the spectrum recorded at 153 K shows that the shift of A band (maximum at 22 600 cm^{-1}) continues below the melting point of butyronitrile (161 K), which proves that dielectric properties of supercooled BTN at temperatures below melting point resemble liquid BTN. A drop in dielectric constant of solid BTN on further decrease of temperature manifests in a blue shift of A band (e.g., band maximum at 23 600 cm^{-1} in the spectrum recorded at 133 K).

Luminescence spectra of CVL in BTN with fluorescence and phosphorescence bands resolved, together with those of 6-DMAPd and MGL, recorded at 77 K are shown in Figure 7. The luminescence spectrum of CVL consists of one fluorescence band with the maximum at 24 000 cm^{-1} and a phosphorescence band as a shoulder on the long-wave side of the luminescence spectrum. The fluorescence band resembles closely that of 6-DMAPd in BTN at 77 K but is red-shifted by 700 cm^{-1}. The phosphorescence spectrum is virtually identical with that of 6-DMAPd but differs significantly both in position of the maximum and in spectral width from the phosphorescence spectrum of MGL in BTN (Figure 7) proving that phosphorescence of CVL is emitted from the triplet state localized on

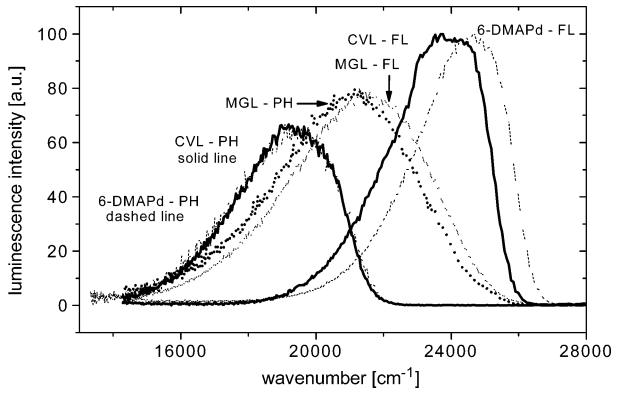

Figure 7. Low-temperature luminescence spectra of CVL, 6-DMAPd and MGL recorded at 77 K in butyronitrile: total luminescence spectra (solid lines) and phosphorescence spectra recorded with choppers (short-lived fluorescence rejected, dashed lines).

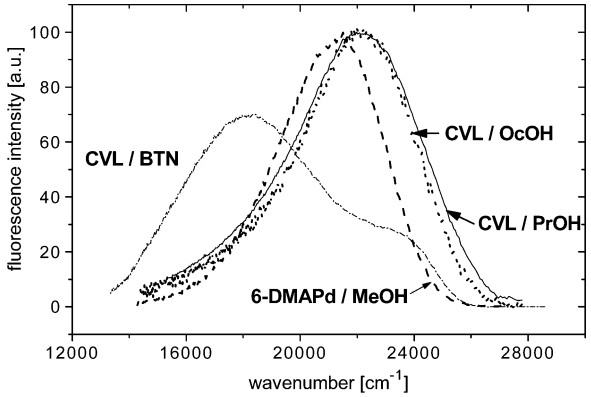

Figure 8. Fluorescence spectra of CVL in 1-propanol and 1-octanol at room temperature compared with fluorescence spectrum of 6-DMAPd in methanol and CVL in BTN.

TABLE 3: Absorption and Fluorescence Data for CVL in Alcohols

solvent	$\tilde{\nu}_{abs}$ [cm^{-1}]	$\tilde{\nu}_{fl}$ [cm^{-1}]	Φ_{fl}	τ_{fl} [ns]
methanol	27800	22250	0.0005	< 0.3
1-propanol	27950	22150	0.0027	< 0.4
1-butanol	27950	22170	0.004	
1-octanol	28000	22150	0.021	1.3

6-DMAPd, which is the lowest triplet state in CVL in low polar environment. Fluorescence and phosphorescence emitted by MGL at low-temperature come from CT singlet and triplet excited states.[11]

3.5. Absorption and Fluorescence in Alcohols. Absorption spectra of CVL in alcohols are similar to those in aprotic solvents (Figure 1) and the solvatochromic shifts of the first absorption band are equivalent to the shifts in aprotic solvents of corresponding polarity (Table 3). The fluorescence of CVL in alcohols is, however, very weak and its quantum yield and decay time strongly depend on the length of aliphatic chain in the alcohol molecule. Fluorescence spectra of CVL in 1-propanol and 1-octanol are compared with that of 6-DMAPd in methanol (and with CVL spectrum in BTN) in Figure 8.

The spectra consist essentially of one broad band and a tail on the long-wave side of the band. Increasing alcohol polarity did not result in any larger solvatochromic shift of the band maximum, indicating that the dipole moment change in the emitting state is significantly less than that in aprotic solvents, and subsequently, that the CVL emission in alcohols originates from a state with different electronic structure than those in polar aprotic solvents. In addition, Stokes shifts for alcoholic solvents

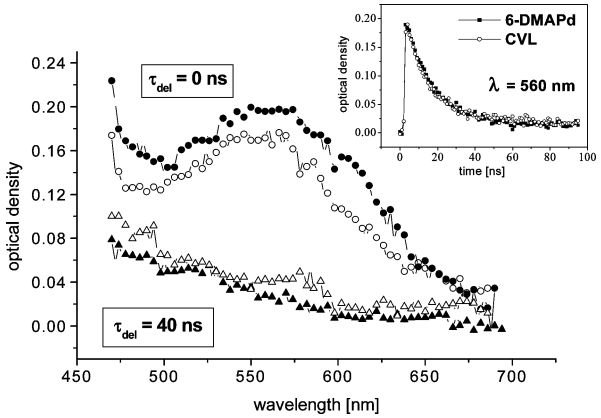

Figure 9. Transient absorption spectra and decays (insert) of CVL (open symbols) and 6-DMAPd (solid symbols) in butyl ether recorded at 0 ns delay (circles) and 40 ns (triangles) after the excitation pulse.

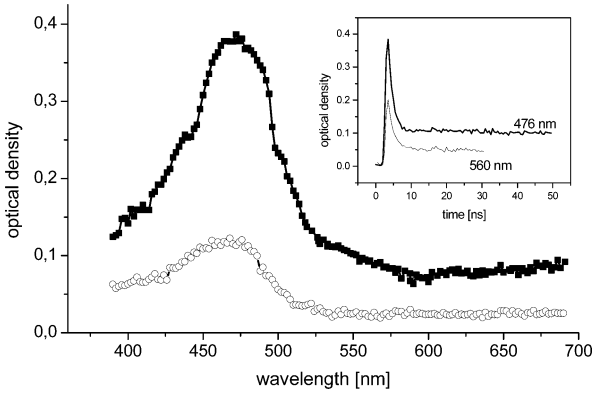

Figure 10. Transient absorption spectra and decays (insert) of a 4.3 $\times$ 10^{-3} M solution of CVL in acetonitrile recorded at 0 ns (solid squares) and at 20 ns (open circles) delay time. Insert shows transient absorption kinetic curves recorded at 476 nm and at 560 nm (multiplied in the insert by 2 for better presentation).

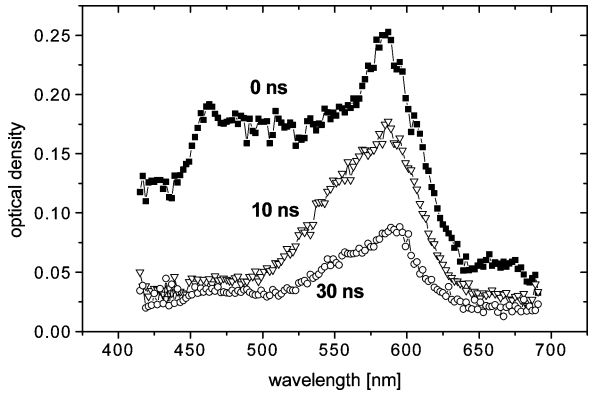

Figure 11. Transient absorption spectra of CVL in *n*-propanol recorded at 0 ns (solid squares), 10 ns (open triangles), and 30 ns (open circles) delay times.

are larger than those of the A band in aprotic solvents of corresponding polarity. The fluorescence quantum yields of CVL in alcohols (Table 3) are drastically reduced as compared with 6-DMAPd in alcohols (0.25 in methanol) and markedly lower than the fluorescence quantum yields of CVL in aprotic solvents of comparable polarity (cf. Table 1).

Further indication for a rapid deactivation processes in CVL in alcohols are very short fluorescence lifetimes, for some of which only upper limit estimates could be determined in measurements on the subnanosecond time scale. All the data suggest completely different mechanism of excited-state processes in alcohols as compared with aprotic solvents.

3.6. Transient Absorption Measurements. *Low and Medium Polar Aprotic Solvents.* Transient absorption (TA) spectra were recorded (i) at the moment the probing pulse coincided (0 ns delay) with the excitation pulse and (ii) at the time the probing pulse was delayed enough to consider the concentration of the S_1 states to be negligible. For quantitative comparisons, both CVL and 6-DMAPd solutions used for TA measurements had the same ground state absorption at the excitation wavelength and approximately the same laser energy was used to excite the samples.

TA spectra of CVL and 6-DMAPd in dibutyl ether[78] recorded at 0 ns delay are very similar (Figure 9).[79] The decay times of transient absorption for both compounds (Figure 9, insert) are equal to those measured for fluorescence and prove that the observed spectrum of CVL is to be ascribed to $S_1 \rightarrow S_n$ transitions localized on 6-DMAPd moiety. The spectra recorded 40 ns after the excitation pulse are also similar for CVL and 6-DMAPd indicating that CVL in low polar solvents undergoes ISC to the local triplet of 6-DMAPd. Kinetic curves of transient absorption recorded in spectral region with more intensive $T_1 \rightarrow T_n$ absorption indicate more efficient ISC in 6-DMAPd as a component of CVL molecule, than in 6-DMAPd standalone, under conditions where ^1CT_B state is energetically not accessible (see Supporting Information). This result indicates that the enhancement in nonradiative deactivation of CVL in low polar solvents, as compared with 6-DMAPd, is to be ascribed mainly to enhanced ISC in CVL.

Highly Polar Aprotic Solvents. Transient absorption spectra and decay curves of CVL in acetonitrile are shown in Figure 10. The spectrum recorded at 0 ns is completely different from that obtained for CVL in BE and consists essentially of a large band with maximum at 472 nm, and a tail extending from 520 to 590 nm. TA kinetic curves recorded at the band maximum (476 nm) and in the tail region (560 nm) indicate rapid (on the ns scale) relaxation to a long living nonemitting state. The decay time ($\sim$1.5 ns) is equal to the fluorescence decay time, pointing out that the spectrum observed at 0 ns delay comes from both emitting singlet states of CVL molecule, hereinafter referred to as $S_1 \rightarrow S_n$ absorption, where S_1 and S_n denote corresponding excited states of both forms. The large band in the $S_1 \rightarrow S_n$ spectrum of CVL in ACN agrees very well with that of the radical cation of dimethylaniline (DMA)[80] proving radical ion pair nature of the ^1CT_B state, whereas the tail may originate either from the ^1CT_A state or from 6-DMAPd radical anion. The spectrum recorded after complete decay of both emitting singlet states (e.g., after 20 ns) has almost identical spectral shape as that recorded at 0 ns delay, and consists essentially of one band matching the large band observed in the $S_1 \rightarrow S_n$ spectrum, with a slight blue shift (band maximum at 468 nm). The spectrum recorded at 20 ns delay agrees well with TA spectrum of CVL in ACN recorded 6 μs after excitation[20] and has been assigned to $T_1 \rightarrow T_n$ transitions. The spectral similarity of $S_1 \rightarrow S_n$ and $T_1 \rightarrow T_n$ absorption spectra strongly suggests identical electronic structure of the ^1CT_B singlet state and the triplet state populated in ACN and in view of the similarity with the spectrum of DMA radical ion leads to conclusion that the charge separation in the ^1CT_B state is still maintained in the triplet state. The triplet states of CVL are not discussed here in detail and the discussion is postponed to future paper.

Transient Absorption in Protic Solvents. TA spectra of CVL in *n*-propanol are shown in Figure 11 (TA decay curves of CVL in *n*-propanol are shown in the Supporting Information). The spectrum recorded at 0 ns delay consists essentially of two bands

with significantly different decay profiles. The band between 440 and 520 nm decays with a decay time approximately equal to that of CVL fluorescence in *n*-propanol (Table 3), and TA in that spectral region can be attributed to $S_1 \rightarrow S_n$ transitions in CVL molecule. On the other hand, the band with the maximum at 586 nm, which is also built up during the excitation pulse, decays more slowly and can be fitted with one decay time ($\tau = 28$ ns). The spectrum observed after the decay of the S_1 state (10 ns after the excitation) is virtually identical with that of the ground-state absorption of the crystal violet cation[81] indicating rapid cleavage of C−O bond in CVL molecule and formation of transient species with electronic structure characteristic for triphenylmethane ionic dye. No measurable rise time on the ns scale was detected for the band at 586 nm which means that the species are built up much faster than 1 ns and, consequently, that the rate of their formation is much larger than that of fluorescence. This strongly indicates that the ionic species must be a product of a rapid photochemical process involving protic solvent molecules and occurring not in equilibrated fluorescing S_1 state but in a vibronically nonrelaxed state, e.g., the ^1CT_B state formed from primarily populated ^1CT_A state.

IV. Discussion

Additive Photophysics of CVL. Molecular structure of crystal violet lactone is set up around a tetrahedral carbon atom with three substituents assembled on four bonds: two DMA rings and 6-DMAPd unit built up on two bonds incorporated in the lactone cycle. Crystal structure study of CVL revealed that the two DMA rings make dihedral angles of 119° and 93° with flat 6-DMAPd and 69° with each other.[82] The lengths of all of the C−C bonds of the central carbon are almost equal (1.514−1.518 Å) which indicates that the delocalization of electrons from aromatic rings does not extend to the central carbon atom. It is the lactone ring which distinguishes CVL from other CV leuco derivatives, e.g., leuconitrile (CVCN), leucoether ($CVOCH_3$), or carbinol (CVOH), where each substituent is attached via one bond to the central carbon atom. Electronic structures of these leuco forms can be considered as superpositions of four nearly noninteracting moieties and the UV absorption spectrum of CVCN or CVOH is virtually a nondistorted sum of transitions localized on DMA groups.[29,30,83] No additional CT absorption transition could be identified in MGL, where the emitting ^1CT state is populated upon excitation localized on one of the DMA groups.[11] Also the absorption spectrum of CVL can be regarded as a superposition of the 6-DMAPd spectrum with those of dimethylaniline/dimethyltoluidine (DMA/DMT), proving that tetrahedral arrangement of structural subunits in CVL effectively weakens their interactions in the ground state. The substitution of the phthalide aromatic ring with dimethylamino group lowers the energy of the lowest excited state in CVL (reached in absorption) significantly below the S_1 energy level of DMA, which substantially differs CVL from MGL. In low-polar solvents[84] CVL relaxes to the lowest excited $S_1(\pi,\pi^*)$ state localized on 6-DMAPd unit. On the other hand, CVCN in low polar solvents displays fluorescence with spectral distribution, quantum yield, and rate constant characteristic for those of $S_1(\pi,\pi^*)$ state localized on DMA moieties.[34] Similar assignments were also reported for leuconitriles of other triarylmethanes.[30,32,85] Contrary to that, the emitting ^1CT state in MGL already in low polar solvents lies below the S_1 states of insulated structural subunits (DMA − above 30200 cm^{-1} and Pd above 35700 cm^{-1}).[11]

Low Polar Solvents. Considerable solvatochromic shifts indicate that the $S_0 \rightarrow S_1$ transition within 6-DMAPd moiety involves significant charge redistribution (displacement) resulting in formation of a polar excited state ^1CT_A directly in absorption transition, similarly as in insulated 6-DMAPd molecule[40] (optical ET). The increase of Stokes shifts of the A band with increasing solvent polarity (Table 1) indicates that the ^1CT_A state is more strongly stabilized by interactions with solvent molecules than the ground state. Linear dependence of Stokes shifts vs solvent polarity function (i.e., $hc(\tilde{\nu}_{abs} - \tilde{\nu}_{fl}(A))$ vs $f'(\epsilon, n) = (\epsilon - 1)/(2\epsilon + 1) - (n^2 - 1)/(2n^2 + 1))$ and moderate value of its intercept (0.4 eV), imply that no substantial conformational change accompanies excited state relaxation in weakly polar solvents. Fluorescence quantum yields for CVL are lower than those for 6-DMAPd but generally follow their change with solvent polarity. Radiative rate constants are similar in both compounds, indicating that the differences in quantum yields result from enhanced nonradiative deactivation of the ^1CT_A state in CVL consisting in higher yield of local triplet formation. An ISC to the triplet state localized on DMA subunit was reported for CVCN.[29]

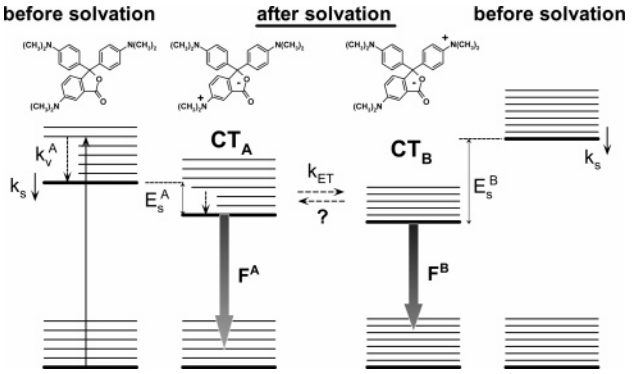

Figure 12. Energy levels of CVL excited states before and after solvation of the molecule. k_s denotes the solvation rate constant, E_s^A and E_s^B are solvation energies of ^1CT_A and ^1CT_B. states, respectively, k_v^A is the rate constant of vibrational relaxation and k_{ET} is the rate constant of electron transfer. F_A and F_B denote fluorescence from ^1CT_A and ^1CT_B state, respectively.

Highly Polar Solvents. Substantial modification of CVL photophysics in medium and highly polar solvents is related to availability of another, lower lying excited singlet state. Dual fluorescence appears in CVL above specific solvent polarity threshold (ϵ between 7.6 and 8.9) and originates from two different excited singlet states: (i) a moderately polar ^1CT_A state localized on 6-DMAPd subunit and (ii) a highly polar ^1CT_B state with electron transferred from one of the DMA groups to 6-DMAPd moiety, analogous to that populated in MGL or in phenolphthalein (PP),[12] differing structurally from MGL by replacement of DMA groups with phenol ones. The ^1CT states in MGL or in PP lie below excited states localized on either of their chromophores and are populated even in nonpolar solvents.[11,12] Recent femtosecond pump−probe study has shown that in MGL excited to the S_2 state, both the $S_2 \rightarrow S_1$ electronic relaxation and the charge separation are completed within 130−150 fs. Phenol radical cation formed upon ET in PP excited to S_1 state appears within 50 fs,[12] and roughly the same value can be assumed for the ET process in MGL excited to the S_1 state. These time constants show that the ET process in LTAMs occurs on the time scale of inertial solvation dynamics and point to a significant role of a purely intramolecular driving force and mechanism of the primary photophysical process.

CVL Energetics and Population of the ^1CT_B State. Excited-state processes in CVL are summarized in the energy diagram in Figure 12. In a vacuum and in low polar solvents, the ^1CT_B

SCHEME 2

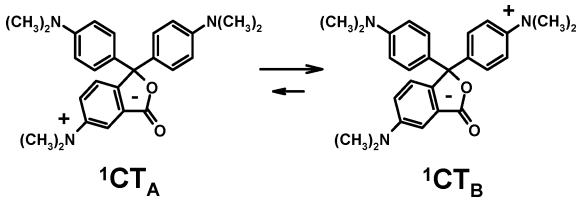

state lies above ^1CT_A and is not accessible from the latter. Necessary stabilization of ^1CT_B under higher polarity conditions is provided by solvation of a large dipole (25.2 D) formed in ET process from one of the DMA groups to 6-DMAPd moiety. The stabilization by solvent polarity leads first to gradual approaching and subsequently to inversion of ^1CT_A and ^1CT_B states. Appropriate ΔG gained upon solvation is, however, only a necessary condition for ^1CT_B population and must be accompanied by favorable charge-transfer kinetics. The latter condition seems to be met if we assume that intrinsic intramolecular ET process resulting in population of the ^1CT_B state in CVL is approximately as fast as that in MGL or PP, i.e., on the sub-100 fs time scale. No detectable rise time in appearance of B fluorescence on the subnanosecond time scale indicates that the ^1CT_B state is formed in very fast process competing with vibrational relaxation of the ^1CT_A state and probably taking place effectively before the latter is completed. In this picture the ^1CT_B state is becoming accessible during solvation of both ^1CT_A and ^1CT_B states[86] and vibrational relaxation of the ^1CT_A state. The kinetics of ^1CT_B population should then be governed by the solvation process and in fact a strong correlation between solvation dynamics and conversion of ^1CT_A into ^1CT_B state has been found.[87] Similar rapidly establishing dynamical interconversion between LE and CT states has been recently proposed by Kovalenko et al. as a critical, rate-determining step in photoinduced ET in bianthryl.[88] Differences in solvation dynamics times[89] and possibly in electrophilic or nucleophilic properties among solvents of comparable polarity may lead to different population distributions of ^1CT_A and ^1CT_B states, and finally to different fluorescence quantum yields from the ^1CT_B state under isopolar conditions (section 3.4). The transition of ^1CT_A to ^1CT_B state may be viewed as a conversion between two differently polar structures with negative charge localized on the lactone ring and positive charge switching between two differently situated dimethylaniline groups (Scheme 2) and possibly with a solvent dependent activation energy barrier of the conversion process. In highly polar solvents the solvent-equilibrated ^1CT_B state is stabilized significantly below the ^1CT_A level, which results in energy activation barrier for the reverse $^1CT_A \leftarrow {}^1CT_B$ reaction, making $^1CT_A \rightarrow {}^1CT_B$ transition irreversible. The formation of the ^1CT_B state may be considered as an adiabatic transformation ("quenching") of the ^1CT_A state due to ET from DMA to 6-DMAPd with formation of an intramolecular exciplex, resembling the ET processes occurring faster than orientational (diffusive) solvation both in intra-[90,91] and in intermolecular[92,93] charge-transfer reactions involving dimethylaniline as electron donor.

The free energy change for the ET reaction populating the ^1CT_B state, $\Delta G°$, can be evaluated from Weller equation[94]

$$\Delta G° = -E_{00} + E(D^+/D^0) - E(A^0/A^-) - E_{ip} \qquad (3)$$

where E_{00} is the energy difference between the S_0 and S_1 states, $E(D+/D^0)$ is the oxidation potential of the electron donor, $E(A^0/A^-)$ is the reduction potential of the electron acceptor, and E_{ip} is the ion pair stabilization energy, estimated from equation $E_{ip} = e^2/\epsilon_s d_{IP}$, where e is the electron charge, ϵ_s is the dielectric constant of the solvent, and d_{IP} is the distance between the donor and the acceptor moiety. As the donor (DMA) and the acceptor (6-DMAPd) are covalently linked to each other, d_{IP} was estimated as a center-to-center distance between DMA and the lactone ring (4.3 Å, the same d_{IP} value was used for MGL[11]). Since the exact $E(A^0/A^-)$ value for 6-DMAPd is not known, the value $E(A^0/A^-) = -2.22$ eV for phthalide[95] has been used, based on the fact that (i) it is basically the phthalide moiety which serves as the electron acceptor in CVL and furthermore (ii) the introduction of meta-substituent does not significantly change the reduction potential of substituted benzene.[96] Then, using the values $E(D+/D^0) = 0.79$ eV for DMA[97] and $E_{00} = 3.50$ eV,[98] one obtains for acetonitrile $\Delta G° = -0.59$ eV.

According to theories describing dynamic solvent effect in ET reactions occurring under nonequilibrium conditions,[99−101] such a $\Delta G°$ value would result in ET reaction rates near the maximum of the flattened[102] "bell shaped" curve depicting the dependence of ET rate on $\Delta G°$, i.e., in the region where the ET processes are predicted to occur in very low energy-barrier or barrierless regime. In models based on such theories the transition to the final state is accomplished along a trajectory that is determined by both the solvent and intramolecular degrees of freedom which act as the ET accepting modes. Very fast ET rates found for MGL and PP[12] combined with the above energetics of ^1CT_B state population indicate that intrinsic ET dynamics in CVL is determined mainly by intramolecular vibrational motions and not by the orientational (diffusive) solvation process, the latter being necessary only to approach ^1CT_B to ^1CT_A. So fast ET dynamics require large interaction between electronic and vibrational motions which in LTAMs is provided by C−O bond in the lactone ring. Gas-phase electron scattering experiments have demonstrated that low energy electron capture by phthalide molecule results in selective excitation of C−O stretching vibrations in Pd anions (Pd^-) being formed, leading to C−O bond instability and even high probability of its cleavage[95,103] The population of vibrationally excited Pd^- strongly suggests preferable deposition of electron energy excess into that specific vibrational mode via a nuclear-excited Feshbach resonance. The latter would indicate possible formation of a dipole-bound Pd^- anion with excess electron weakly bound by a long-range electrostatic field generated by a high (4.9 D) dipole moment of Pd molecule[104] and residing on a very diffuse orbital outside the molecular frame.[105] The overlap of this orbital with the orbital of primary excited donor part of the LTAM molecule may result in their coupling and lead to high ET rates observed in these systems. Theoretical work is needed to explore the occurrence and role of such dipole-bound resonance states. Possible photoinduced C−O bond dissociation in the lactone ring is discussed at the end of this section.

Comparison with Other Leuco Forms. Other leuco forms of triarylmethanes also undergo solvent polarity induced alteration of photophysics.[34] In leuconitriles, an increase in solvent polarity above a certain threshold results in a dramatic decrease of fluorescence quantum yields and lifetimes and opens a new deactivation channel linked to photodissociation of the C−CN bond. The process is initiated by dissociative intramolecular electron transfer from one of the DMA groups to the CN group[33] and results in detachment of the latter. Solvent polarity induced photodissociation of leuconitriles is relatively slow (0.1−5 ns in MGCN) and occurs from the thermally equilibrated level of the S_1 state.[32] In CVL, solvent polarity

SCHEME 3

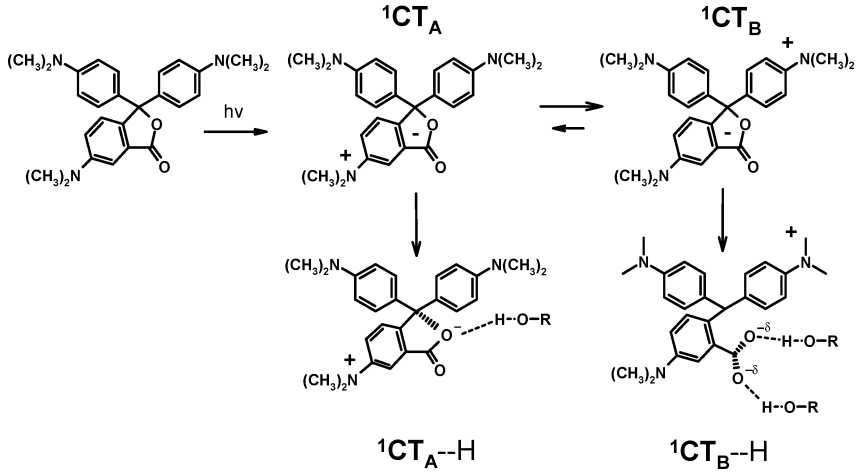

also stabilizes the final state of the ET process (^1CT_B), making the latter accessible from ^1CT_A state. Fast kinetics of ^1CT_B state formation and its dependence on solvent longitudinal dielectric relaxation time[87] strongly indicate that the intrinsic ET process in CVL must proceed much faster than in leuconitriles and takes place from a vibronically (or even solvationally) nonequilibrated ^1CT_A state.

Charge Recombination in Highly Polar Solvents. Decreasing quantum yields and decay times of A and B fluorescences with growing solvent polarity (Table 1) point to an effective, solvent polarity-dependent nonradiative deactivation mechanism that becomes operative in line with decreasing energy of the ^1CT_B state. Stabilization of ^1CT_B energy in the solvation process does not only enable the CVL molecule to relax to the ^1CT_B state but also, due to increasing proximity to the ground state, provides an additional deactivation channel. Since the yield of the ^1CT_B state formation in CVL could not be exactly determined, the spectroscopic characteristics of the ^1CT_B state are not known and the discussion of its nonradiative decay must largely rely on decay kinetics of the structurally analogous ^1CT state in MGL where the yield of the ^1CT state formation was determined to be 100%.[11] We believe that the similarity of the ^1CT state in MGL and the ^1CT_B state in CVL fully justifies such considerations. Low fluorescence transition dipole moments of the ^1CT state in MGL at room temperature point to the forbidden character of radiative transition from the ^1CT state and substantial part of MGL molecules deactivates from ^1CT via efficient, solvent polarity dependent nonradiative process, with radiative rate, k_r, remaining nearly polarity-independent. Strong temperature dependence of nonradiative deactivation includes substantial contribution from temperature dependence of solvent polarity. Similar observations have been made for CVL. Direct radiationless charge recombination between DMA^+ and Pd^- moieties is the most probable mechanism of the enhanced nonradiative deactivation of ^1CT state in MGL. Intrinsic reason for the effect is the dependence of the nonradiative rate constant, k_{nr}, on the energy of ^1CT state (being strongly affected by solvent polarity). Solvent polarity induced radiationless deactivation of ^1CT_B state in CVL may thus, by analogy, be rationalized by appealing to the energy gap law.[106] The decreasing energy gap between the ^1CT_B state and the ground state induces increasing efficiency of the direct CR process due to exponentially increasing Franck−Condon factors and leads to higher rate of radiationless decay. Similar effects were observed in excited intramolecular CT state deactivation of donor−acceptor carbazole derivatives,[53] for aryl derivatives of aromatic amines[107] and in nonradiative electron transfer in contact ion pairs.[108]

Lactone Ring Opening and CVL Photophysics in Alcohols. The similarity of CVL absorption spectra in aprotic solvents and in alcohols proves that also in protic media the electronic excitation promotes CVL to the ^1CT_A state localized on the 6-DMAPd moiety. Different fluorescence spectra and very low fluorescence quantum yields suggest that subsequent photophysical processes in CVL in alcohols are completely different than those in aprotic solvents. A strong dependence of fluorescence quantum yield on the length of aliphatic chain in alcohol molecule, and therefore on its hydrogen bonding ability, points to important role of proton transfer from alcohol to excited CVL molecule. Alcohols are both polar and hydrogen-bonding media, and a combination of these two properties is of substantial importance for CVL photophysics and photochemistry. First, alcohol polarity provides energetic stabilization of the ^1CT_B vs ^1CT_A state, similarly as in aprotic media of equivalent polarity, and gradual approaching of the ^1CT_A state by ^1CT_B and subsequent inversion of the states with increasing polarity can be expected. Before, however, the ^1CT_B state will become accessible, so before the solvent fully solvates CVL molecule in ^1CT_A state, the latter has a chance to relax adiabatically on the excited-state surface via formation of a hydrogen bond with the solvent (fluorescent ^1CT_A- -H state in Scheme 3), and the molecules that "managed" to form a hydrogen bond in that time display fluorescence with the spectrum similar to that of 6-DMAPd in alcohols (Figure 8). Upon sufficient stabilization by alcohol polarity, the ^1CT_B state becomes accessible from the ^1CT_A state and an electron is transferred from DMA to 6-DMAPd. The electron transfer results in the formation of a vibrationally excited 6-DMAPd anion ($6\text{-}DMAPd^-$) and the energy gained upon ET is preferentially deposited in C−O bond vibrations. Under excitation of that vibrational mode $6\text{-}DMAPd^-$ passes from initial geometry to a geometry with stretched C−O bond that, especially under favorable conditions, e.g. possibility of hydrogen bonding, can finally break heterolytically resulting in opening of the lactonic ring. In this picture, the electron is transferred upon the ^1CT_B state population prior to dissociation, and its transfer provides activation energy needed to break the bond. Such a photoinduced heterolytic dissociation can be adiabatic, with preservation of excitation as in lactone forms of rhodamins,[8−10] or it can be a diabatic process leading to the formation of a CVL zwitterion in the ground state. Observation of transient species with electronic structure characteristics for triphenylmethane dye cation in ns transient absorption spectra

that are formed in a process taking place in much less than 1 ns, so not being the products of deactivation of the CVL emitting state, proves that the species are formed in a direct diabatic dissociation channel of C−O bond (nonfluorescent ^1CT_B- -H state in Scheme 3) starting from the ^1CT_B state. So, these two deactivation channels in protic solvents originate from two excited states of CVL (Scheme 3): the excited-state emitting fluorescence is formed before the solvation has stabilized the ^1CT_B state, so that it becomes accessible from the ^1CT_A state, whereas the diabatic channel consists of ultrafast C−O dissociation in the ^1CT_B state. The lactone ring is closed on the time scale of tens of ns. A more detailed study is required to gain a deeper insight into the photophysics and especially photochemistry of CVL in protic media. It is to be noted here that our work does not provide any evidence for photoinduced homolytic diabatic C−O bond cleavage in CVL followed by biradical formation in aprotic acetonitrile.[20] On the contrary, we did not observe either any ground-state ionic species nor the appearance of color upon irradiation of CVL in ACN.

V. Conclusions

Based on comparison with two molecules mimicking structural subunits of CVL (6-DMAPd and MGL), dual fluorescence of crystal violet lactone in *aprotic* solvents has been ascribed to come from two polar excited states, one of which (^1CT_A) is localized within the 6-DMAPd part of the molecule, whereas the other (^1CT_B) is populated after ET from one of the dimethylaniline groups on the 6-DMAPd moiety. The ^1CT_B state becomes accessible and is populated in a very fast excited state process. The medium plays a critical role in CVL photophysics, with solvent polarity affecting the energetics of both excited states and controlling availability of various deactivation pathways, and solvent dielectric properties possibly influencing the kinetics of primary excited-state processes. In *protic* solvents CVL shows completely different behavior with formation of crystal violet cation following solvent assisted heterolytic cleavage of C−O bond in lactone ring.

Remarkable solvatochromism of CVL both in low and in highly polar aprotic solvents, CVL sensitivity to protic environment and its ability to undergo large, solvent polarity-driven charge redistribution in the excited state (probably without marked structural changes) suggest potential applications of CVL as an interesting probe of polarity and proticity in various microenvironments. The ability of CVL to report these properties of local microenvironment combined with a possibility of switching between single and dual luminescence can be modified by changing the energy gap between ^1CT_A and ^1CT_B states via appropriate substituents at phthalide moiety.

Acknowledgment. This work was supported by grant 3T09A05418 from the Committee of Scientific Research (KBN).

Supporting Information Available: Solvatochromic plots of absorption maxima for CVL and 6-DMAPd. Detailed description of higher absorption bands. Mirror symmetry of absorption and emission bands in CVL and 6-DMAPd. Details of spectral decomposition procedure for fluorescence spectra. Transient absorption kinetics of CVL in BE and PrOH. This material is available free of charge via the Internet at http://pubs.acs.org.

References and Notes

(1) Grabowski, Z. R.; Rotkiewicz, K.; Rettig, W. *Chem. Rev.* **2003**, *103*, 3899 and references therein.

(2) Lippert, E.; Lüder, W.; Boos, H. In *Advances in molecular spectroscopy*; Mangini, A., Ed.; Pergamon Press: Oxford, U.K., 1962; p 443.

(3) Rotkiewicz, K.; Grellmann, K. H.; Grabowski, Z. R. *Chem. Phys. Lett.* **1973**, *19*, 315.

(4) Grabowski, Z. R.; Rotkiewicz, K.; Siemiarczuk, A.; Cowley, D. J.; Baumann, W. *Nouv. J. Chim.* **1979**, *3*, 443.

(5) Rettig, W. *Angew. Chem., Int. Ed. Engl.* **1986**, *25*, 971.

(6) Turro, N. J.; McVey, J.; Ramamurthy, V. Lechtken, P. *Angew. Chem., Int. Ed. Engl.* **1979**, *18*, 572.

(7) Milota F.; Warmuth, C.; Tortschanoff, A.; Sperling, J.; Fuhrmann, T.; Salbeck, J.; Kauffmann, H. F. *Synth. Met.* **2001**, *121*, 1497.

(8) Klein, U. K. A.; Hafner, F. W. *Chem. Phys. Lett.* **1976**, *43*, 141.

(9) Grigoryeva, T. M.; Ivanov, V. L.; Nizamov, N.; Kuzmin, M. G. *Dokl. Akad. Nauk* **1977**, *232*, 1108.

(10) Karpiuk, J.; Grabowski Z. R.; De Schryver, F. C. *J. Phys. Chem.* **1994**, *98*, 3247.

(11) Karpiuk, J. *Phys. Chem. Chem. Phys.* **2003**, *5*, 1078.

(12) Bizjak, T.; Karpiuk, J.; Lochbrunner, S.; Riedle, E. *J. Phys. Chem. A* **2004**, *108*, 10763.

(13) (a) Karpiuk, J. *Ann. Polish Chem. Soc.* **2001**, 271. (b) Karpiuk, J.; Contribution presented at *XVIIIth IUPAC Symposium on Photochemistry*; Dresden, 2000, Book of Abstracts; p 335.

(14) (a) Oster, G.; Nishijima, Y. *J. Am. Chem. Soc.* **1956**, *78*, 1581. (b) Förster, Th.; Hoffmann G. *Z. Phys. Chem. NF* **1971**, *75*, 63.

(15) Vogel, M.; Rettig, W.; Heimbach, P. *J. Photochem. Photobiol. A* **1991**, *61*, 65.

(16) (a) Changenet, P.; Plaza, P.; Martin, M. M.; Meyer, Y. H., Rettig, W. *Chem. Phys.* **1997**, *221*, 311. (b) Changenet, P.; Plaza, P.; Martin, M. M.; Meyer, Y. H. *J. Phys. Chem. A* **1997**, *101*, 8186.

(17) National Cash Register, U.S. Patent 2,417,897 [CA 41, 7416a].

(18) Koertum, G.; Vogel, J. *Chem. Ber.* **1960**, *93*, 706.

(19) White, M. A. *J. Chem. Edu.* **1998**, *75*, 1119.

(20) Kaneko, Y.; Neckers, D. C. *J. Phys. Chem. A* **1998**, *102*, 5356.

(21) Nag, A. K. *Indian J. Chem. Sect. A.: Inorg., Bio-inorg., Phys., Theor. Anal. Chem.* **1994**, *33*, 658.

(22) Ma., Y.; Zhu, B.; Wu, K. *Solar Energy* **2001**, *70*, 417. Ma., Y.; Zhang, X.; Zhu, B.; Wu, K. *Solar Energy* **2002**, *72*, 511.

(23) Duxbury, D. F. *Chem. Rev.* **1993**, *93*, 381 and references therein.

(24) Ishikawa, M.; Ye, J. Y.; Maruyama, Y.; Nakatsuka, H. *J. Phys. Chem. A* **1999**, *103*, 5629.

(25) Fletcher, I. J.; Zink, R. In *Chemistry and Application of Leuco Dyes*; Muthyala, R., Ed.; Plenum Press: New York, 1997; p 97.

(26) Allen, N. S.; Hughes, N.; Mahon, P. *J. Photochem.* **1987**, *37*, 379.

(27) Takaoka, K.; Maeda, S.; Miura, H.; Endo, K.; Chong, D. P. *Bull. Chem. Soc. Jpn.* **1998**, *71*, 807.

(28) Holmes, E. O., Jr. *J. Phys. Chem.* **1966**, *70*, 1037.

(29) Herz, M. L. *J. Am. Chem. Soc.* **1975**, *97*, 6777.

(30) Geiger, M. W.; Turro, N. J.; Waddell, W. H. *Photochem. Photobiol.* **1977**, *25*, 15.

(31) Manring, L. E.; Peters, K. S. *J. Phys. Chem.* **1984**, *88*, 3516.

(32) Spears, K. G.; Gray, T. H.; Huang, D. *J. Phys. Chem.* **1986**, *90*, 779.

(33) Miller, R. M.; Spears, K. G.; Gong, J. H.; Wach, M. *J. Phys. Chem.* **1994**, *98*, 1376.

(34) Jarikov, V. V.; Neckers, D. C. *J. Org. Chem.* **2001**, *66*, 659. For a recent review, see: Jarikov, V. V.; Neckers, D. C. *Adv. Photochem.* **2001**, *26*, 1.

(35) Irie, M. *J. Am. Chem. Soc.* **1983**, *105*, 8858.

(36) Wan, P.; Yates, K.; Boyd, M. K. *J. Org. Chem.* **1985**, *50*, 2881.

(37) Minto, R. E.; Das, P. K. *J. Am. Chem. Soc.* **1989**, *111*, 8858.

(38) Gurzadyan, G. G.; Steenken, S. *Chem. Eur. J.* **2001**, *7*, 1808.

(39) Lipson, M.; Deniz, A. A.; Peters, K. S. *J. Phys. Chem.* **1996**, *100*, 3580. Lipson, M.; Deniz, A. A.; Peters, K. S. *J. Am. Chem. Soc.* **1996**, *118*, 2992. Lipson, M.; Deniz, A. A.; Peters, K. S. *Chem. Phys. Lett.* **1998**, *288*, 781.

(40) Karpiuk, J.; Svartsov, Y. N.; Nowacki, J. manuscript in preparation.

(41) Fischer, O. *Chem. Ber.* **1879**, *12*, 1685.

(42) Stanetty, P.; Rodler, I.; Krumpak, B. *J. Prakt. Chem.* **1993**, *335*, 17.

(43) Velapoldi, R. A. National Beaureau of Standards 378, Proc. Conf. NBC, Gaithersburg, 1972; p 231.

(44) Eaton, D. F. *Pure Appl. Chem.* **1988**, *60*, 1107.

(45) Jasny, J. *J. Lumin.* **1978**, *17*, 143.

(46) Jasny, J.; Sepioł, J.; Karpiuk, J.; Gilewski, J. *Rev. Sci. Instrum.* **1994**, *65*, 3646.

(47) It is to be noted that laser irradiation (under the same conditions) of CVL solution in acetonitrile which was in contact with air for a longer time (e.g., from a bottle opened many times) resulted in appearance of a broad band with a maximum at 610−612 nm. A similar band was reported by Kaneko and Neckers (ref 20, Figure 6, continuous line spectrum). In the present paper the band was not observed after irradiation of a CVL solution prepared using ACN from a freshly opened bottle.

(48) Kuzuya, M.; Miyake, F.; Okuda, T. *Chem. Pharm. Bull.* **1983**, *31*, 791.

(49) Beilaits, I. L.; Nurmukhametov, R. N. *Zh. Fiz. Khim.* **1970**, *44*, 29.

(50) Böttcher, C. J. F. In *Theory of Electric Polarization*; Van Belle, O. C., Bordewijk, P., Rip, A., Eds.; Elsevier: Amsterdam, 1973; Vol. 1.

(51) Discussion of solvent effects on absorption bands requires referencing in advance to some results and questions discussed in detail in relation to the solvent effects on emission bands and excited-state dipole moments considerations in sections 3.2 and 3.3 of the paper.

(52) Liptay, W. In *Excited states*; Lim, E. C., Ed.; Academic Press: New York, 1974; p 129.

(53) (a) Kapturkiewicz, A.; Herbich, J.; Karpiuk, J.; Nowacki, J. *J. Phys. Chem.* **1997**, *101*, 2332. (b) Kapturkiewicz, A.; Herbich, J. *J. Am. Chem. Soc.* **1998**, *120*, 1014.

(54) Onsager, L. *J. Am. Chem. Soc.* **1936**, *58*, 1486.

(55) The term "shoulder" is used because the overlap of the second absorption band with subsequent (third) band does not allow one to determine the exact position of the band maximum.

(56) Karpiuk, J. Ph.D. Thesis, Institute of Physical Chemistry, Polish Academy of Sciences, Warsaw, 1996.

(57) The notation of the short-wave fluorescence band with "A" and long-wave fluorescence band with "B" follows the sequence the bands appear with increasing solvent polarity and is reverse to the nomenclature used to designate the long-wave band in dual luminescence spectrum of dimethylaminobenzonitrile (DMABN) ("A" for anomalous fluorescence), ref 2. In view of the molecular structure of CVL, the long-wave luminescence cannot be termed "anomalous" one.

(58) Assuming reasonable requirement that quantum yield determinations are to be carried out under conditions with sample absorption matching that of the standard at the wavelength of excitation, high absorbance of CVL solution studied in ref 20 (the concentration given in that paper would correspond to $A \approx 1.6$ at 365 nm with 1 cm optical path way) would require comparably high absorption of rhodamine B solution used as a fluorescence quantum yield standard ("an actinometer"). Low molar absorption coefficient at 365 nm of the latter would additionally increase the required concentration of rhodamine B to approximately 8×10^{-4} M^{-1} involving significant problems with concentration dependent equilibria between different ionic forms of rhodamine B and consequently the dependence of rhodamine B fluorescence quantum yield on concentration. See Kubin, R. F.; Fletcher, A. N. *J. Luminesc.* **1982**, *27*, 455.

(59) Marcus, R. *J. Phys. Chem.* **1989**, *93*, 3078.

(60) Lewis, J. E.; Maroncelli, M. *Chem. Phys. Lett*. **1998**, *282*, 197.

(61) The position of the long-wave absorption band of the **Z** form of CVL should be very close to that of crystal violet cation, which in ethanol occurs at 590 nm, see ref 23.

(62) Waluk, J.; Pakuła, B.; Bałakier, G. *Chem. Phys. Lett.* **1983**, *94*, 58.

(63) Mukherjee, S.; Chattopadhyay, A.; Samanta, A.; Soujanya, T. *J. Phys. Chem.* **1994**, *98*, 2809.

(64) (a) Lippert, E. *Z. Naturforschg.* **1955**, *10a*, 541. (b) Mataga, N.; Kaifu, Y.; Koizumi, M. *Bull. Chem. Soc. Jpn.* **1955**, *28*, 690.

(65) Beens, H.; Knibbe, H.; Weller, A. *J. Chem. Phys.* **1967**, *47*, 1183.

(66) Soujanya, T.; Fessenden, R. W.; Samanta, A. *J. Phys. Chem.* **1996**, *100*, 3507.

(67) (a) Rechthaler, K.; Köhler, G. *Chem. Phys.* **1994**, *189*, 99. (b) Schneider, F.; Lippert, E. *Ber. Bunsen-Ges. Physik. Chem.* **1968**, *72*, 1155; **1970**, *74*, 624.

(68) 3.0 Å is half of the distance between the amino nitrogen atom and the oxygen atom in the lactone ring for optimized AM1 ground-state geometry, and $4.1 \text{ Å} = 0.4(x + r_C + r_O)$, where x is the distance between carbon atom from methyl group attached to amino nitrogen and the oxygen in the lactone ring in 6-DMAPd, setting the long axis of the 6-DMAPd molecule, and r_C and r_O are van der Waals radii of those atoms, respectively.

(69) Details of the calculation will be published in ref 40.

(70) For $a = 4.1$ Å, the values $\mu_e = 11.6$ D and $\alpha = 26°$ have been obtained.

(71) Baumann, W.; Bischof, H.; Fröhling, J.-C.; Brittinger, C.; Rettig, W.; Rotkiewicz, K. *J. Photochem. Photobiol. A* **1992**, *64*, 49.

(72) Kanya, R.; Ohshima, Y. *Chem. Phys. Lett.* **2003**, *370*, 211.

(73) AM1 estimation gave $\mu_g = 5.5$ D.

(74) On assumption that the changes in solvent refraction index can be neglected.

(75) Interpolation formula according to the data from Janelli, L.; Lopez, A.; Silvestri, L. *J. Chem. Eng. Data* **1983**, *28*, 166, 169.

(76) Reichardt, C. *Solvent effects in organic chemistry*; Verlag Chemie: Weinheim, Germany, 1979; p 270.

(77) The temperature-dependent fluorescence spectra have been measured in 20 K intervals, so the temperature values given here are only indicative for the phenomena described in this work.

(78) CVL solubility in nonpolar hydrocarbons (e.g., hexane) was not enough to ensure CVL (or MGL) concentration that would be sufficient for transient absorption measurements.

(79) In the present version of our nanosecond spectrophotometer, transient absorption transient spectra could not be reliably recorded in spectral regions with very high fluorescence intensity as the fluorescence (and also the probing light) had to be masked to a large extent with cut off filters.

(80) Shida, T. *Electronic absorption spectra of radical ions*; Elsevier: New York, 1988.

(81) Sundström, V.; Gillbro, T.; Bergström, H. *Chem. Phys.* **1982**, *73*, 439.

(82) Theocharis, C. R.; Jones, W. *J. Crystal. Spectrosc. Res.* **1984**, *14*, 121.

(83) Sporer, A. H. *Trans. Faraday Soc.* **1961**, *57*, 983.

(84) For the purposes of the following discussion, all aprotic solvents used in present work have been divided into *low polar* solvents and *polar* ones. The first group includes the solvents, in which CVL shows single short-wave fluorescence at room temperature, i.e., from hexane to THF, and the other group includes those, in which CVL displays dual luminescence.

(85) Brown, F. G.; Cosa, J. *Chem. Phys. Lett.* **1977**, *45*, 429.

(86) The solvation process of the ^1CT_A state and its time dependence cannot be neglected.

(87) Karpiuk, J.; Schmidhammer, U.; Lochbrunner, S.; Riedle, E. contribution presented at 68. Physikertagung der Deutschen Physikalischen Gesellschaft, 2004, Munich, Germany; manuscript in preparation.

(88) Kovalenko, S. A.; Pérez Lustres, J. L.; Ernsting, N. P.; Rettig, W. *J. Phys. Chem. A* **2003**, *107*, 10228.

(89) Horng, M. L.; Gardecki, J. A.; Papazyan, A.; Maroncelli, M. *J. Phys. Chem.* **1995**, *99*, 17311.

(90) Tominaga, K.; Walker, G. C.; Jarzęba, W.; Barbara, P. F. *J. Phys. Chem.* **1991**, *95*, 10475.

(91) Pandurski, E.; Fiebig, T. *Chem. Phys. Lett.* **2002**, *357*, 272.

(92) Yoshihara, K.; Tominaga; K.; Nagasawa, Y. *Bull. Chem. Soc. Jpn.* **1995**, *68*, 696.

(93) Castner E. W., Jr.; Kennedy D.; Cave, R. J. *J. Phys. Chem. A* **2000**, *104*, 2869.

(94) Rehm, D.; Weller, A. *Isr. J. Chem.* **1970**, *8*, 259.

(95) Vincent, M. L.; Peters, D. G. *J. Electroanal. Chem.* **1992**, *327*, 121.

(96) Kemula, W.; Krygowski, T. M. In *Encyclopedia of electrochemistry of the elements*; Bard, A. J., Lund, H., Eds.; Marcel Dekker: New York, 1979; Vol. XIII.

(97) Bourget, D.; Jacques, P.; Vauthey, E.; Suppan, P. Haselbach, E. *J. Chem. Soc., Faraday Trans.* **1994**, *90*, 2481.

(98) E_{00} was assumed to be equal to the spectral position of the shoulder in CVL absorption spectrum in hexane (28200 cm^{-1}).

(99) Sumi H.; Marcus, R. A. *J. Chem. Phys.* **1986**, *84*, 4894.

(100) Jortner, J.; Bixon, M. *J. Chem. Phys.* **1988**, *88*, 167.

(101) Walker, G. C.; Åkesson, E.; Johnson, A. E.; Levinger, N. E.; Barbara, P. F. *J. Phys. Chem.* **1992**, *96*, 3728.

(102) (a) Kapturkiewicz, A. In *Advances in Electrochemical Science and Engineering*; Alkire, R. C., Gerischer, H., Kolb, D. M., Tobias, Ch. W., Eds.; Wiley-VCH: Weinheim, Germany, 1997; Vol. 5. (b) Gould, I. R.; Young, R. H.; Moody, R. E.; Farid, S. *J. Phys. Chem.* **1991**, *95*, 2068.

(103) Zykov, B. G.; Vasil'ev, Y. V.; Fal'ko, V. S.; Lachinov, A. N.; Khvostenko, V. I.; Gileva, N. G. *JETP Lett.* **1996**, *64*, 439.

(104) Wallmark, I.; Krackov, M. H.; Chu, S.-H.; Mautner, H. G. *J. Am. Chem. Soc.* **1970**, *90*, 4447.

(105) Desfrancois C.; Abdoul-Carime H.; Schermann J.-P. *Int. J. Mod. Phys. B* **1996**, *10*, 1339.

(106) (a) Turro, N. J. *Modern Molecular Photochemistry*; Benjamin/Cummings: New York, 1978. (b) Michl, J.; Bonačič-Koutecky, V. *Electronic Aspects of Organic Photochemistry*; Wiley-Interscience: New York, 1990.

(107) Herbich, J.; Kapturkiewicz, A. *Chem. Phys.* **1991**, *158*, 143. Herbich, J.; Kapturkiewicz, A. *Chem. Phys.* **1993**, *170*, 221.

(108) Gould, I. R.; Noukakis, D.; Gomez-Jahn, L.; Young, R. H.; Goodman, J. L. Farid, S. *Chem. Phys.* **1993**, *176*, 439.